

# Behavioral patterns and mean-field games in epidemiological models

Finnegan Buckley<sup>1</sup> and Alexander Vladimirs<sup>2</sup>

<sup>1</sup>Department of Mathematics, Cornell University, Ithaca, NY, [ftb24@cornell.edu](mailto:ftb24@cornell.edu)

<sup>2</sup>Department of Mathematics and Center for Applied Mathematics, Cornell University, Ithaca, NY, [vladimirsky@cornell.edu](mailto:vladimirsky@cornell.edu)

December 24, 2025

## Abstract

We introduce a new type of Mean Field Game epidemiological models, in which subpopulations have different behavioral patterns: some are viewed as “highly rational” (choosing Nash-equilibrium long-term strategies) while others follow pre-specified “non-rational” patterns (e.g., either sticking to their usual habits or trying to mimic those around them). Our model also allows for occasional behavioral switches, which rational individuals also take into account when formulating their Nash-equilibrium strategies. While this modeling approach is general, here we develop it for individuals choosing their “contact rates” within a particular Susceptible-Infected-Recovered-Susceptible-Dead (SIRSD) epidemics model. The latter is based on a frequency-based force of infection and the mortality rate that rapidly increases once the proportion of infected individuals exceeds some prescribed threshold, resulting in a strain on medical resources. Numerical tests illustrate the properties of our model and highlight the ways in which additional/non-rational behavioral patterns and behavioral switching increase the impact of infectious diseases. The paper aims to build a bridge between two distinct communities of epidemiological modelers and to promote the consideration of behavioral patterns in broader Mean Field Games literature.

## 1 Introduction

Mathematical epidemiology is a classical area of applied mathematics, which saw a significant increase in research activities since the onset of COVID pandemic. Many mathematicians seized the opportunity to bring new tools and ideas to these problems of obvious and immediate societal importance. Among them, the experts in Mean Field Games (MFGs) have proposed a number of models

to explain individuals' choices on how much to follow official rules and recommendations (on vaccinations, social distancing, mask wearing, etc) [1, 2, 5, 6, 10, 14, 40, 42]. In MFG literature, these choices are viewed as fully rational in a selfish or decentralized manner: "optimal" from the point of view of individual decision makers, but often quite far from "socially-optimal". While obviously an important contribution, such models do not account for the fact that people are not uniform in their priorities, rationality, analytic abilities, consistency in carrying out their preliminary plans, and self-awareness. Our goal in this paper is to show how MFG-type models can be extended to address some of these limitations, and to explore the effect of such features in the context of epidemiology.

The importance of population heterogeneity and behavioral patterns is widely recognized in modeling the spread of infectious diseases. Many of the classical models already split population into multiple groups based on their frailty and propensity to spread the infection. E.g., the need to consider the role of super-spreader *core groups* separately is a particularly common feature in modeling sexually-transmitted diseases [21]. But more recent behavior-epidemiology models go much further, allowing for individuals' occasional switches in behavioral patterns, and modeling how the frequency of such switches is affected by individuals' fatigue from following the rules, peer pressure, and changing epidemiological situation; see, for example, [9, 16, 29, 30, 31, 32, 35, 36]. However, in all these models, the list of behavioral patterns is pre-specified, parameters within each pattern (e.g., the contact rate of each sub-population) remain fixed in time, and individuals are assumed to switch between these patterns/sub-populations purely stochastically with prescribed rates and without any attempt to explain why each subpopulation adopts their set of parameter values. This makes it harder to use such models in the context of public policy; e.g., in predicting how people's behavior (and the resulting epidemiological trajectory) will change in response to proposed guidance updates.

The game-theoretic framework is, in many ways, the opposite of the above phenomenological approach, with individual behavior typically explained through the lens of maximizing one's personal "rewards" or "returns". When many individuals (or "players") make their decisions independently while affecting each other, the concept of optimality has to be replaced by the notion of Nash equilibrium: a combination of individual decisions/strategies such that no individual can improve their personal returns by unilaterally changing their own strategy. But computing and analyzing Nash

equilibria is generally harder in dynamic games involving a large number of players. Mean Field Games (MFGs) were introduced to address the latter challenge [22, 26, 27] and have by now found much success, particularly in economics and engineering applications. The key idea in MFGs is to consider a game with *infinitely many* “small” players, each of whom interacts with an evolving density of players rather than with specific individual players<sup>1</sup>. Computationally, this leads to a coupled system of differential equations describing the evolution of players’ density and players’ optimal (Nash equilibrium) behavior. For MFGs over a finite state space, this yields a two point boundary value problem for a system of Ordinary Differential Equations (ODEs) [19]. This is a natural fit for epidemiological models, where possible individual states are based on their current health status (e.g., Susceptible, Infected, Recovered, or Dead – giving rise to “SIRSD compartment models”) and where the ODEs typically arise as a large population limit of interacting Markov chains.

The rational optimization perspective allows for comparing the epidemiological and economic impact of Nash equilibrium solutions (when individuals make independent decisions) with what could be achieved with “socially optimal” solutions (if everyone followed the optimally formulated official guidance, recovered in the framework of Mean Field Control) [10, 40]. Other models go beyond this comparison and formulate the problem as a “Stackelberg game” between the authorities, who choose a public policy under assumption that people will respond to them in a rational but selfish manner, and individuals, who react to that known public policy by pursuing Nash equilibrium personal strategies [2]. While the above are usually formulated with the assumption that the logic of all participants is homogeneous, there is also a broader literature on *multipopulation MFGs* [4, 11, 13], which allows each subpopulation to have different optimization goals and dynamics. Such features are obviously useful in epidemiological context; e.g., for elderly/frail individuals, the rate of death while infected is usually higher and the frequency of interactions between different age groups is often non-uniform as well [1].

---

<sup>1</sup>To avoid a possible terminological confusion, we note explicitly that MFGs are very different from “games against the field,” which were introduced much earlier by John Maynard Smith as a part of the Evolutionary Game Theory (EGT) [41]. In contrast with EGT models, in MFGs (1) each player has state (quite distinct from their strategy); (2) the game is dynamic (lasting over a long or infinite horizon), with each player’s state changing as a result of their personal strategy, the evolving distribution of all players’ states and, in some cases, of strategies adopted by all others; and (3) the strategies are not inherited but chosen rationally (in a time-dependent way) to minimize the cost accumulated over time. In MFGs, what a player chooses to do now depends on predicted consequences; in EGT, all changes to the composition of strategies are driven by the current composition and the current strategy “payoffs” only.

But the full rationality and consistency assumptions remain fundamental even in such standard MFG-multipopulation models, with all individuals assumed to have the full knowledge of others' priorities and risks, ability to compute a personal (time-dependent) Nash equilibrium strategy, also predicting how similar optimization carried out by others will influence the epidemiological situation long term, and consistency in implementing the selected Nash strategy throughout the course of epidemic. This idealized description is hardly fitting for most humans, and the resulting discrepancies can have significant consequences if a Stackelberg-optimal public policy is adopted in practice.

In this paper, we suggest an approach for relaxing several of these assumptions by recognizing that only some of the people are highly rational, while others frequently adopt behavioral patterns that are not grounded in game theory. More specifically, we consider three subpopulations: Reckless/stubborn individuals, who largely ignore the epidemiological situation; Followers/consensus-seekers, who try to adopt the “population-averaged” behavior; and rational Optimizers, who make their decisions strategically in an MFG-fashion, taking the behavior of all subpopulations into account. Because many people are inconsistent in carrying out their long-term plans, in our model we also allow for individual’s occasional random switching among these behavioral patterns, with switching rates possibly dependent on the epidemiological situation or fatigue from restricting their contacts.

Since the goal of the paper is largely to foster the dialogue between two distinct research communities, this also influences our exposition: we primarily focus on fundamental modeling assumptions and their consequences illustrated through numerical experiments, leaving other important aspects (theoretical, numerical, and data-centric) for the future. To make the discussion concrete, we introduce a specific simple SIRSD ODE model in § 1.1. We then develop its generalized MFG version in § 2: starting with the optimization task faced by a single rational individual when others' strategies are already known, deriving a Nash description when all such individuals make decisions simultaneously, then adding other behavioral subpopulations and the possibility of switching between them. The numerical results based on this general model are presented in § 3. The limitations and directions for future work are discussed in § 4.

### 1.1 The baseline SIRSD model.

We assume that at any given time each individual can be either Susceptible (S), Infected (I), Recovered/Immune (R) or Dead (D), with the corresponding letters also used to encode the fraction of individuals in each state. For the sake of simplicity, we also ignore the births and disease-unrelated deaths. We further assume that

- Susceptible, Infected, and Recovered individuals each on average contact  $c_s$ ,  $c_i$ , and  $c_r$  other individuals (respectively) per unit time. For now, these will be treated as constants, but starting in the next section we will interpret these as individual's time-dependent control variables.
- $\beta$  is the probability of infectious disease transmission for each contact of a Susceptible with any Infected individual.
- The overall probability of a Susceptible becoming Infected per contact is thus

$$p = \underbrace{\beta}_{\mathbb{P}(\text{infection upon contacting an infected})} \frac{\overbrace{c_i I}^{\text{Fraction of contacts made by Infected}}}{c_s S + c_i I + c_r R} \quad (1)$$

This formula is consistent with a frequency-based force of infection and the so-called *proportionate mixing* assumption [20, 33]. Models built using a frequency-based force of infection are increasingly found to be appropriate for a broad range of infectious diseases; see, for example [17, Table 1].

- $(1/\mu)$  is the average time one stays infected until recovery; we will thus refer to  $\mu$  as the recovery rate.
- As the immunity starts to wane,  $(1/\gamma)$  is the average time one stays immune after recovery; we will thus refer to  $\gamma$  as the immunity waning rate.
- $\delta(I)$  is the (monotone non-decreasing) per capita death rate of Infected due to the disease. We use this dependence on  $I$  to model the possible strain on medical services and infrastructure due to high infection levels. While our general framework does not depend on a specific  $\delta(I)$ , in all of the following experiments we use a cubic spline-based death rate to model a jump from

$\delta_1 \geq 0$  (when hospitals are operating normally) to  $\delta_2 \geq \delta_1$  (when hospitals are overwhelmed by Infected):

$$\delta(I) = \begin{cases} \delta_1, & \text{if } I \leq d_1; \\ \delta_1 + (\delta_2 - \delta_1) \left( \left( \frac{I-d_1}{d_2-d_1} \right)^2 \left( 3 - 2 \left( \frac{I-d_1}{d_2-d_1} \right) \right) \right), & \text{if } d_1 \leq I < d_2; \\ \delta_2, & \text{if } I \geq d_2. \end{cases} \quad (2)$$

Using this notation and assumptions, the progression of epidemics can be found by solving a system of ODEs

$$S' = \underbrace{-pc_s S}_{\text{new infections}} + \underbrace{\gamma R}_{\text{waning immunity}} \quad (3)$$

$$I' = \underbrace{pc_s S}_{\text{new infections}} - \underbrace{\mu I}_{\text{recoveries}} - \underbrace{\delta(I) I}_{\text{new deaths}} \quad (4)$$

$$R' = \underbrace{\mu I}_{\text{recoveries}} - \underbrace{\gamma R}_{\text{waning immunity}} \quad (5)$$

$$D' = \underbrace{\delta(I) I}_{\text{new deaths}} \quad (6)$$

for  $t \in (0, T]$ , starting from the initial conditions  $S(0) = S_0$ ,  $I(0) = I_0$ ,  $R(0) = R_0$ ,  $D(0) = D_0$ .

The table 1 summarizes our baseline parameter values and initial conditions. These are used throughout the paper except where different values are specified explicitly.

An epidemic trajectory resulting from this model is illustrated in Figure 1 using the baseline contact rates ( $c_s = 5$ ,  $c_i = 3$ ,  $c_r = 5$ ), which will be motivated in the next section, starting from the initial conditions  $D_0 = R_0 = 0$ ,  $I_0 = 5 \times 10^{-3}$ ,  $S_0 = 1 - I_0$ , and computing until  $T = 200$ . This Figure tells an SIRSD-typical story with an initial growth in Infecteds reaching the maximum by  $t \approx 18.4$ , leading to an increase in the number of Recovereds up to  $t \approx 45.6$ ; then the waning immunity leading to another local maximum in the number of Susceptibles by  $t \approx 94.5$  and a subsequent second (much smaller) increase in the number of Infecteds around  $t \approx 120$ . Since the death rates are relatively low,

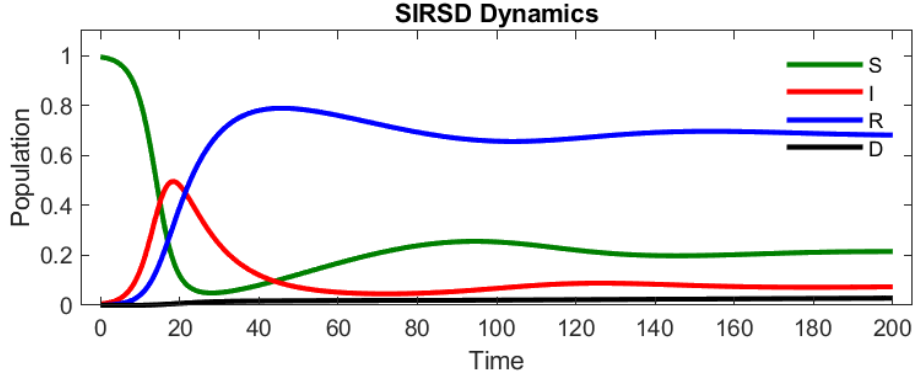
Initial Condition	Value	Parameter	Description	Value
$S_0$	0.995	$\gamma$	Rate of loss of immunity	1/90
$I_0$	0.005	$\mu$	Rate of recovery	0.1
$R_0$	0	$\beta$	Chance of infection upon contact with infected	0.15
$D_0$	0			

Parameter	Description	Value
$\delta_1$	Low mortality rate (when $I < d_1$ )	0.001
$\delta_2$	High mortality rate (when $I > d_2$ )	0.002
$d_1$	Maximum $I$ for the low mortality regime	0.15
$d_2$	Minimum $I$ for the high mortality regime	0.25
$V_D$	The death penalty	-100

**Table 1:** Baseline values for the initial conditions and ODE parameters.

the total number of dead is  $D(T) \approx 0.0286$ .



**Figure 1:** SIRSD epidemic dynamics over a 200 day time interval

## 2 MFG model with behavioral patterns

Since this manuscript is intended to be of interest to a broader audience of epidemiological modelers, we describe our approach in greater detail than it is usually done in MFG literature, focusing on modeling assumptions as well as on their mathematical and practical implications.

Our focus will be on a mixed population of agents, all of whom change their personal contact rate independently with the full knowledge of current epidemiological situation. Some of these agents (referred to as “Optimizers”) are assumed to be highly rational in a sense that they

- strive to maximize their personal cumulative reward, which is computed by integrating over the time-horizon  $[0, T]$  their *instantaneous utility* function  $u$  that changes based on their current

status (S, I, or R) and the chosen contact rate;

- can predict the future epidemiological trajectory if everyone's current and future contact rates are known;
- can find Nash-equilibrium strategies, reflecting their understanding that all other Optimizers are simultaneously performing their own selfish maximization as well.

The logic of other agents (Reckless or Followers) will be mathematically described later, but we emphasize that they are not viewed as rational in the same sense as Optimizers.

We start by focusing on Optimizers: describing their instantaneous utility functions (§ 2.1), formulating the problem faced by a single Optimizer when everybody else's contact rates are known/fixed (§ 2.2), and explaining how the Nash-equilibrium strategies are obtained in the MFG setting when the entire population consists of Optimizers (§ 2.3). We then finally consider the full/mixed population (§ 2.4), in which the Optimizers take into account both the impact of non-optimizing agents *and* everybody's (including Optimizers') propensity for occasional switches in behavioral patterns.

## 2.1 Utility of Contact Rates

Individuals need to make contact with others for economic gains and for their personal well being. Thus, we assume that an individual's instantaneous utility is a function of their contact rate with others. While our general model does not require a specific type of utility functions, all of the numerical experiments in § 3 are based on the utility functions previously formulated in [10]. For each status  $z \in \{S, I, R\}$  and contact rate  $c$  we use

$$u_z(c) = (b_z c - c^2)^g - a_z, \quad (7)$$

with parameter values  $g = 0.25$ ,  $b_S = b_R = 10$ ,  $b_I = 6$ ;  $a_S = a_R = 0$ , and  $a_I = 4$ . This specifies the same instantaneous utility for all healthy individuals (status  $S$  or  $R$ ) and a different, generally lower, instantaneous utility for Infected individuals; see Figure 2.

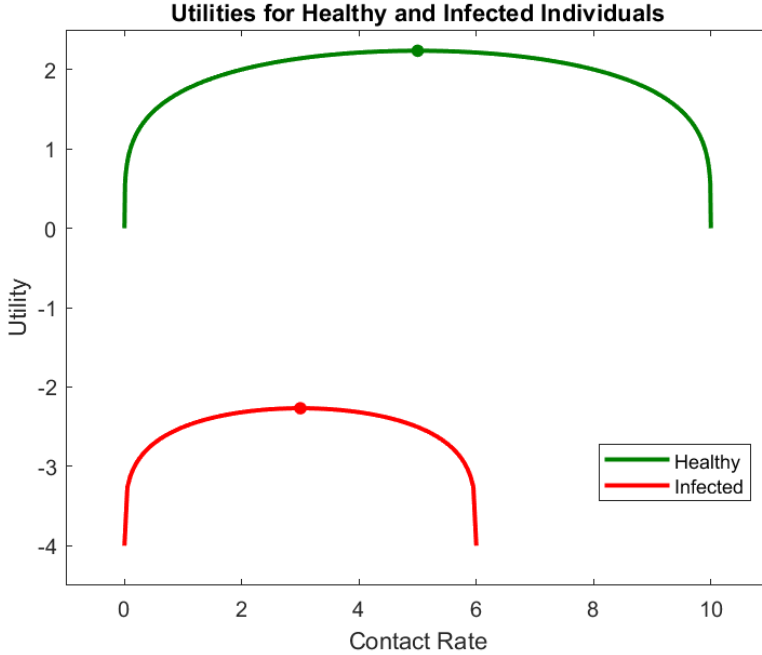


**Figure 2:** Graphs of instantaneous utility functions for a healthy (susceptible or recovered) individual and an infected individual. The maximum values of the two functions are noted by the dots on the corresponding graph, achieved with contact rates  $\bar{c}_R = \bar{c}_S := b_S/2 = b_R/2 = 5$  and  $\bar{c}_I := b_I/2 = 3$  respectively.

These utility functions are concave (as long as the shape parameter  $g$  is in  $(0, 1]$ ) and have a unique maximum in contacts, achieved at  $c = b_z/2$ . Parameter  $a_z$  determines the baseline level of utility gain for individuals in state  $z$ . We naturally enforce  $b_S = b_R > b_I$  and  $a_S = a_R < a_I$  since infected lose economic productivity and suffer an overall health cost. The maximal instantaneous utility values  $\bar{u}_S = \bar{u}_R$  and  $\bar{u}_I$  are achieved with contact rates  $\bar{c}_R = \bar{c}_S := b_S/2 = b_R/2 = 5$  and  $\bar{c}_I := b_I/2 = 3$  respectively. These are also the contact rates chosen in the previous section to produce Figure 1.

## 2.2 Single individual optimizing their Contact Rate Strategy

An individual in the population accumulates reward according to the utility function of their current state, which is subject to random transitions. To begin, suppose that the entire population uses some specific and known contact rate strategy  $\mathbf{c}(t) = (c_S(t), c_I(t), c_R(t))$ , leading to the epidemic trajectory  $\mathbf{y}(t) = (S(t), I(t), R(t), D(t))$ . If a lone focal individual chooses to follow some different strategy  $\hat{\mathbf{c}} = (\hat{c}_S(t), \hat{c}_I(t), \hat{c}_R(t))$ , they will not influence the course of the epidemic (i.e.,  $\mathbf{y}(t)$  will

remain the same). But they will change their personal chances of getting ill and their personal lifestyle. Mathematically, for a focal individual starting from a state  $\xi \in \{S, I, R, D\}$  at the time  $t < T$  and using contact rate  $\hat{\mathbf{c}}(\cdot)$  until the time  $T$ , their expected cumulative reward will be

$$\mathcal{J}(\xi, t, \hat{\mathbf{c}}(\cdot); \mathbf{y}(\cdot), \mathbf{c}(\cdot)) = \mathbb{E} \left[ \int_t^{\min(T, T_D)} u_{z(r)} \left( \hat{c}_{z(r)}(r) \right) dr + V_D \mathbf{1}_{T_D \leq T} \right],$$

where  $z(r) \in \{S, I, R, D\}$  is that individual's state at the time  $r \in [t, T]$ , starting from  $z(t) = \xi$  and changing through a continuous in time Markov chain with transition rates based on the current state of epidemics and the chosen contact rates. Here,  $D$  is the absorbing state,  $T_D = \min\{r \geq t \mid z(r) = D\}$  is a random time of death, and  $V_D$  is a large negative terminal "reward" received if this sad outcome occurs within the planning horizon. Some of these transition rates are constant; e.g., for the recovery from infection or the loss of immunity to happen within a short time interval  $\tau$ ,

$$\mathbb{P}(z(r + \tau) = R \mid z(r) = I) = \mu\tau + o(\tau) \quad \text{and} \quad \mathbb{P}(z(r + \tau) = S \mid z(r) = R) = \gamma\tau + o(\tau).$$

Other rates are  $\mathbf{y}(r)$ -dependent or even  $(\mathbf{y}(r), \mathbf{c}(r), \hat{\mathbf{c}}(r))$ -dependent; e.g, for a death to occur within a short time interval  $\tau$ ,  $\mathbb{P}(z(r + \tau) = D \mid z(r) = I) = \delta(I(r))\tau + o(\tau)$  and for a new infection,

$$\mathbb{P}(z(r + \tau) = I \mid z(r) = S) = \hat{c}_s(r) p(\mathbf{y}(r), \mathbf{c}(r))\tau + o(\tau),$$

with  $p$  determined by the current state of the epidemic and the current contact rates used by all others, as defined in (1).

Assuming that the focal individual strives to maximize their expected cumulative reward, one can define *value functions* to quantify the result of optimizing the contact rates:

$$V_\xi(t) = \sup_{\hat{\mathbf{c}}(\cdot)} \mathcal{J}(\xi, t, \hat{\mathbf{c}}(\cdot); \mathbf{y}(\cdot), \mathbf{c}(\cdot)). \quad (8)$$

Here,  $\xi \in \{S, I, R\}$  is again their initial state at the time  $t \leq T$  and  $V_\xi(t)$  is the (optimized) expected cumulative reward in the time remaining until  $T$ . When  $z(r) = I$  or  $z(r) = R$ , the focal individual's choices do not influence their transition rates, and thus they will always choose the contact rate that

maximizes their current utility function:  $\hat{c}_I^* = \bar{c}_I$  and  $\hat{c}_R^* = \bar{c}_R$ , achieving utility values  $\bar{u}_I = u_I(\bar{c}_I)$  and  $\bar{u}_R = u_R(\bar{c}_R)$  respectively; see Figure 2. On the other hand, that individual has a non-trivial choice to make when  $z(r) = S$ : a contact rate lower than  $\bar{c}_S$  is often optimal since it reduces the immediate chances of getting infected. Using the above expressions for transition rates, the optimality equations satisfied by the value functions can be written as

$$V_S(t) = \max_{\hat{c}_S(\cdot)} \left\{ \left( \int_t^{t+\tau} u_S(\hat{c}_S(r)) dr \right) + p\hat{c}_S(t)\tau V_I(t+\tau) + (1-p\hat{c}_S(t)\tau) V_R(t+\tau) \right\} + o(\tau); \quad (9)$$

$$V_I(t) = \int_t^{t+\tau} \bar{u}_I dr + \mu\tau V_R(t+\tau) + \delta(I(t)) \tau V_D + (1 - \mu\tau - \delta(I(t)) \tau) V_I(t+\tau) + o(\tau); \quad (10)$$

$$V_R(t) = \int_t^{t+\tau} \bar{u}_R dr + \gamma\tau V_S(t+\tau) + (1 - \gamma\tau) V_R(t+\tau) + o(\tau); \quad (11)$$

for any starting time  $t < T$  and any  $\tau \leq T - t$ . Here,  $p = p(\mathbf{y}(t), \mathbf{c}(t))$  is again computed by formula (1) based on the current state of epidemics. A standard control-theoretic argument based on a Taylor-series expansion of (9-11) yields a system of ODEs for the value functions

$$V'_S(t) = -u_S(\hat{c}_S^*) + p(\mathbf{y}(t), \mathbf{c}(t)) \hat{c}_S^* (V_S(t) - V_I(t)); \quad (12)$$

$$V'_I(t) = -\bar{u}_I + \mu(V_I(t) - V_R(t)) + \delta(I(t)) (V_I(t) - V_D); \quad (13)$$

$$V'_R(t) = -\bar{u}_R + \gamma(V_R(t) - V_S(t)); \quad (14)$$

satisfied for all  $t \in [0, T]$  with the terminal condition  $V_S(T) = V_I(T) = V_R(T) = 0$ , and the optimal  $(\mathbf{y}(t), \mathbf{c}(t))$ -dependent contact rate while susceptible is

$$\hat{c}_S^* = \arg \max_{\hat{c}_S} \left\{ u_S(\hat{c}_S) + p(\mathbf{y}(t), \mathbf{c}(t)) \hat{c}_S (V_I(t) - V_S(t)) \right\}. \quad (15)$$

### 2.3 Nash Equilibrium: Mean Field Game System

Of course, if all individuals selfishly and rationally choose their contact rate, this will alter the course of the epidemic, with optimality thus replaced by the notion of Nash equilibrium. (Given the constant transition rates from  $I$  and  $R$ , it is easy to see that all rational selfish agents will still use the utility-maximizing contact rates  $\bar{c}_I$  and  $\bar{c}_R$  while Infected and Recovered respectively. But the

choice of optimal contact rate while Susceptible will now become more subtle since it will affect both  $\mathbf{y}(\cdot)$  and their immediate chances of getting Infected.) As usual in MFG literature, we will say that  $\mathbf{c}(t) = (c_s(t), c_l(t), c_r(t))$  and  $\mathbf{y}(t) = (S(t), I(t), R(t), D(t))$  form a Nash equilibrium if

(1)  $\mathbf{y}(t)$  results from  $\mathbf{c}(t)$  via ODEs (3)-(6) and

(2)  $\mathcal{J}(\xi, t, \mathbf{c}(\cdot); \mathbf{y}(\cdot), \mathbf{c}(\cdot)) \geq \mathcal{J}(\xi, t, \hat{\mathbf{c}}(\cdot); \mathbf{y}(\cdot), \mathbf{c}(\cdot))$

for all  $\xi \in \{S, I, R, D\}$ ,  $t \in [0, T]$ , and all contact rate policies  $\hat{\mathbf{c}}(\cdot)$ . The latter condition ensures that no individual has any incentive for switching their personal contact rate.

Using  $p(c_s)$  as a shorthand for

$$p(S, I, R; c_s) = \beta \frac{\bar{c}_l I}{c_s S + \bar{c}_l I + \bar{c}_r R}, \quad (16)$$

the resulting Mean Field Game can be now described by a system of seven ODEs:

$$S' = -p(c_s^*) c_s^* S + \gamma R; \quad (17)$$

$$I' = p(c_s^*) c_s^* S - \mu I - \delta(I) I; \quad (18)$$

$$R' = \mu I - \gamma R; \quad (19)$$

$$D' = \delta(I) I; \quad (20)$$

$$V_s' = -u_s(c_s^*) + p(c_s^*) c_s^* (V_s - V_l); \quad (21)$$

$$V_l' = -\bar{u}_l + \mu(V_l - V_r) + \delta(I)(V_l - V_d); \quad (22)$$

$$V_r' = -\bar{u}_r + \gamma(V_r - V_s); \quad (23)$$

with the Nash contact rate of susceptible individuals specified by

$$c_s^* = \arg \max_{c_s} \left\{ u_s(c_s) + p(c_s) c_s (V_l - V_s) \right\}. \quad (24)$$

**Remark.** To aide the readers less familiar with MFG-type models, we emphasize the distinction, which is obvious for MFG experts. Despite the many similarities, the above model is very different

from the focal-individual discussion in the previous subsection. In §2.2, we assumed that the ODEs (3)-(6) were first solved forward in time using the known contact rates  $\mathbf{c}(t)$  adopted by the entire population. The focal individual was then trying to find a better contact rate policy  $\hat{\mathbf{c}}(t)$  (that would be used by them and them alone) by solving the ODEs (12-14) backward in time with the epidemic trajectory  $\mathbf{y}(t) = (S(t), I(t), R(t), D(t))$  already fixed based on  $\mathbf{c}(t)$ . In contrast, the above ODE system (17-23) is fully coupled via (24) also influencing  $\mathbf{y}(t)$ , and thus should be treated as a Two Point Boundary Value Problem (TPBVP) with initial conditions specified for  $S, I, R, D$  and terminal conditions specified for  $V_S, V_I, V_R$ .

In MFG literature, such systems are often treated numerically by forward-backward iterations, which, for stability reasons, might also be combined with an under relaxation [28] or with the so called “fictitious play” [7]. Since our models in this paper are over a finite state space, we instead employ the standard collocation methods for TPBVPs (e.g., the built-in Matlab function `bvp5c` [25]). The initial guess for the TPBVP solver is generated by solving the “single optimizer problem” (12-14) for the epidemics trajectory corresponding to a population-wide use of the specific contact rate policy  $\mathbf{c}(t) = (\bar{c}_S, \bar{c}_I, \bar{c}_R)$ .

## 2.4 Behavioral patterns and switching

The model described above is close in spirit to others commonly presented in MFG literature. (E.g., a similar approach to SIR/SEIR models but with a density-based force of infection can be found in [10].) We now extend it to reflect three different behavioral patterns, modeled as three distinct subpopulations: Reckless/stubborn, Followers/consensus-seekers, and Optimizers. All of them use the same contact rates while Infected (i.e.,  $\bar{c}_I$ ) or Recovered/Immune (i.e.,  $\bar{c}_R$ ) since these rates maximize their instantaneous utility function and do not influence the rate of transition to other health states. The subpopulations are thus only different in how they choose their contact rates while Susceptible, but we maintain three health compartments ( $S, I$ , and  $R$ ) in each subpopulation separately, using the subscripts ( $r, f$ , and  $o$ ) to distinguish them<sup>2</sup>. The same subscript notation is

---

<sup>2</sup>This is necessary because we do not assume that one’s behavioral pattern/subpopulation changes automatically due to a change in one’s health status: a reckless individual may not become more careful just because they suffered from the infection. In fact, some of the studies show that those recovered from a disease are in some cases more risk-prone afterwards [15, 23, 24].

also used to distinguish the contact rates and the value functions.  $S, I, R$  variables without subscript will now refer to the total number of people in each respective class across all sub-populations; e.g.,  $S = S_r + S_f + S_o$ .

Susceptible Reckless individuals ignore the epidemiological situation and the risk of getting infected, thus selecting the contact rate that myopically maximizes their utility function:  $c_{S,r}(t) = \bar{c}_s$ .

Susceptibles Followers prefer to adopt the “consensus” modeled by averaging the contact rate used by all Susceptibles (across all subpopulations). This averaging will obviously depend on the specific contact rate  $c_{S,o}^*(t)$  selected by the Susceptible Optimizers through the process described below. But for now we simply characterize the Follower’s chosen rate as a function of whatever contact rate  $c$  those Optimizers might be considering:

$$c_{S,f}(c) = \frac{\bar{c}_s S_r + c_{S,f}(c) S_f + c S_o}{S} = \frac{\bar{c}_s S_r + c S_o}{S_r + S_o}, \quad (25)$$

where the second (explicit) expression for  $c_{S,f}(c)$  is valid as long as  $S_r(t) + S_o(t) \neq 0$  (otherwise the Followers don’t have anyone to follow).

Finally, the rational Susceptible Optimizers will select a Nash-type contact rate  $c_{S,o}^*$ , but taking into account two new complications:

1. the behavior of other subpopulations (including the fact that the Followers will be immediately influenced by whatever the Optimizers select) and
2. the possibility that all people (including the Optimizers!) might occasionally change their behavioral patterns in the future. (E.g., an Optimizer becoming Reckless for a while or vice versa.)

We note that the latter reflects a subtle shift in modeling assumptions. In MFG literature, optimizing agents are assumed to be not only fully rational in formulating their Nash-equilibrium strategies, but also fully *consistent* in implementing those strategies long term. Instead, we assume that Optimizers are inconsistent (prone to possible/occasional behavioral switches) and understand that they will follow the rationally chosen strategy only while in that Optimizer mode. They are further assumed

to use this self-awareness when searching for an optimal (Nash-equilibrium) strategy.

To address the first of these complications, we need to modify our formula for computing the per contact probability of becoming infected. Extending (16), we will now use  $p(c)$  as a shorthand for

$$p(S_r, S_f, S_o, I, R; c) = \beta \frac{\bar{c}_I I}{\bar{c}_S S_r + c_{S,f}(c) S_f + c S_o + \bar{c}_I I + \bar{c}_R R}, \quad (26)$$

where  $c$  is the contact rate currently considered by Susceptible Optimizers.

As for the behavioral switches, we assume that they are happening at random times, driven by a nonhomogeneous Poisson process with rates  $\lambda_{j,k}$ , which are possibly dependent on the changing epidemiological situation and the currently used contact rates. More precisely, we assume that for an individual who is currently using a behavioral pattern  $j \in \{r, f, o\}$  the probability of switching to another behavioral pattern  $k \in \{r, f, o\} \setminus \{j\}$  within a short time  $\tau$  is equal to  $\lambda_{j,k}\tau + o(\tau)$ . The fact that  $\lambda_{j,k}$  are not necessarily constant is a natural modeling assumption; e.g., transitions to reckless behavior are less likely when the total number of Infected people is high and more likely when Nash-style rational behavior leads to fatigue or life-style envy (when  $u_s(c_{S,o}^*)$  is much lower than  $\bar{u}_s$ ). For the sake of notational simplicity, we mostly omit these dependencies of  $\lambda_{j,k}$ , though we do keep them in mind in stating the optimization problem. They are also illustrated in some of the computational experiments in §3.

The value function for a Susceptible Optimizer, representing the expected rewards for the remaining time interval  $[t, T]$ , will satisfy the following optimality equation for any sufficiently small  $\tau$ :

$$V_{S,o}(t) = \max_{c_S(\cdot)} \left\{ \left( \int_t^{t+\tau} u_s(c_s(r)) dr \right) + pc_s(t)\tau V_{I,o}(t+\tau) + \lambda_{o,r}\tau V_{S,r}(t+\tau) + \lambda_{o,f}\tau V_{S,f}(t+\tau) + \left( 1 - (pc_s(t) + \lambda_{o,r} + \lambda_{o,f})\tau \right) V_{S,o}(t+\tau) \right\} + o(\tau), \quad (27)$$

where the dependence of  $p$ ,  $\lambda_{o,r}$ , and  $\lambda_{o,f}$  on  $c_s(t)$  are not indicated explicitly to keep the notation manageable. This equation is a generalization of (9), and a similar Taylor series expansion argument

yields an ODE for the value function

$$V'_{S,o} = -u_S(c_{S,o}^*) + p(c_{S,o}^*)c_{S,o}^*(V_{S,o} - V_{I,o}) + \lambda_{o,r}(c_{S,o}^*)(V_{S,o} - V_{S,r}) + \lambda_{o,f}(c_{S,o}^*)(V_{S,o} - V_{S,f}) \quad (28)$$

with the optimal contact rate found from

$$c_{S,o}^* = \arg \max_c \left\{ u_S(c) + c p(c)(V_{I,o} - V_{S,o}) + \lambda_{o,r}(c)(V_{S,r} - V_{S,o}) + \lambda_{o,f}(c)(V_{S,f} - V_{S,o}) \right\}. \quad (29)$$

The resulting model can be now formally described by a system of 19 coupled ODEs using indices  $j \in \{r, f, o\}$  and  $k \in \{r, f, o\} \setminus \{j\}$  :

$$S'_j = -p(c_{S,o}^*) c_{S,j} S_j + \gamma R_j + \sum_{k \neq j} (\lambda_{k,j} S_k - \lambda_{j,k} S_j); \quad (30)$$

$$I'_j = p(c_{S,o}^*) c_{S,j} S_j - \mu I_j - \delta(I) I_j + \sum_{k \neq j} (\lambda_{k,j} I_k - \lambda_{j,k} I_j); \quad (31)$$

$$R'_j = \mu I_j - \gamma R_j + \sum_{k \neq j} (\lambda_{k,j} R_k - \lambda_{j,k} R_j); \quad (32)$$

$$D' = \delta(I) I; \quad (33)$$

$$V'_{S,j} = -u_S(c_{S,j}) + p(c_{S,o}^*) c_{S,j} (V_{S,j} - V_{I,j}) + \sum_{k \neq j} \lambda_{j,k} (V_{S,j} - V_{S,k}); \quad (34)$$

$$V'_{I,j} = -\bar{u}_I + \mu (V_{I,j} - V_{R,j}) + \delta(I) (V_{I,j} - V_D) + \sum_{k \neq j} \lambda_{j,k} (V_{I,j} - V_{I,k}); \quad (35)$$

$$V'_{R,j} = -\bar{u}_R + \gamma (V_{R,j} - V_{S,j}) + \sum_{k \neq j} \lambda_{j,k} (V_{R,j} - V_{R,k}); \quad (36)$$

where  $c_{S,r} = \bar{c}_S$ ,  $c_{S,o} = c_{S,o}^*$  is specified by formula (29), and  $c_{S,f} = c_{S,f}(c_{S,o}^*)$  is specified by formula (25). For the sake of readability, we do not explicitly list above the dependency of behavioral switching rates  $\lambda$  on  $c_{S,o}^*$  and  $I$ . This is again a TPBVP, with initial conditions specified for  $(S_j, I_j, R_j)_{j \in \{r, f, o\}}$  and  $D$ , while zero terminal conditions are assumed for  $(V_{S,j}, V_{I,j}, V_{R,j})_{j \in \{r, f, o\}}$ .

### 3 Results

We note that the model summarized by equations (30-36) is fairly broad. In particular, with the fully Reckless population and no behavioral switches (i.e.,  $S_k(0) = I_k(0) = R_k(0) = 0$  and  $\lambda_{r,k} = 0$  for all  $k \in \{f, o\}$ ) it reduces to the traditional SIRSD model described in §1.1 and illustrated in Figure 1. We begin by comparing it with the other extreme case: the “traditional MFG” scenario – a fully rational population of Optimizers and no behavioral switches (i.e.,  $S_k(0) = I_k(0) = R_k(0) = 0$  and  $\lambda_{o,k} = 0$  for all  $k \in \{r, f\}$ ), illustrated in Figure 3. In both cases, we use the time horizon  $T = 100$  and start with 0.5% of population Infected and all others initially Susceptible. The middle graph shows that Optimizers, acting independently and optimizing their contact rates selfishly, still manage to flatten the curve of the epidemic and to reduce the peak number of Infected. While it is not obvious from the graphs, there is also a reduction in the total number of deaths: from 2.08% in a fully Reckless population to 1.58% in a population consisting of fully rational Optimizers. This is achieved through a reduction in Susceptible Optimizers’ contact rate (bottom row of Figure 3), which varies with the danger (based on the current number of Infected) and the time remaining until  $T$ . We note that the increase in contact rate towards the end (and the corresponding slight increase in Infected) is due to our imposing no terminal penalty ( $V_{s,j}(T) = V_{i,j}(T) = V_{r,j}(T) = 0$ ,  $j \in \{r, f, o\}$ ), particularly due to the lack of penalty for still being infected by the time  $T$ . This modeling simplification might be justifiable if a cure is under development and will definitely become available at the time  $T$ . In general, using a negative  $V_{i,j}(T)$  is perhaps more realistic, but we have chosen these zero terminal conditions here to make a comparison with prior modeling results (e.g., those in [10]) easier.

#### 3.1 Sensitivity to parameters in behaviorally homogeneous populations

Before introducing interacting sub-populations, we compare the sensitivity of the epidemic trajectory to parameter variations in these same two “homogeneous population” scenarios: Reckless only (or the original SIRSD model, i.e.,  $S_k(0) = I_k(0) = R_k(0) = 0$  and  $\lambda_{r,k} = 0$  for all  $k \in \{o, f\}$ ) and Optimizers only (i.e.,  $S_k(0) = I_k(0) = R_k(0) = 0$  and  $\lambda_{o,k} = 0$  for all  $k \in \{r, f\}$ ).

We first vary the initial proportion of infected in the population; see Figure 4. In both cases, increasing  $I_0$  causes higher and earlier peaks in infections. Comparing the two scenarios, the peaks

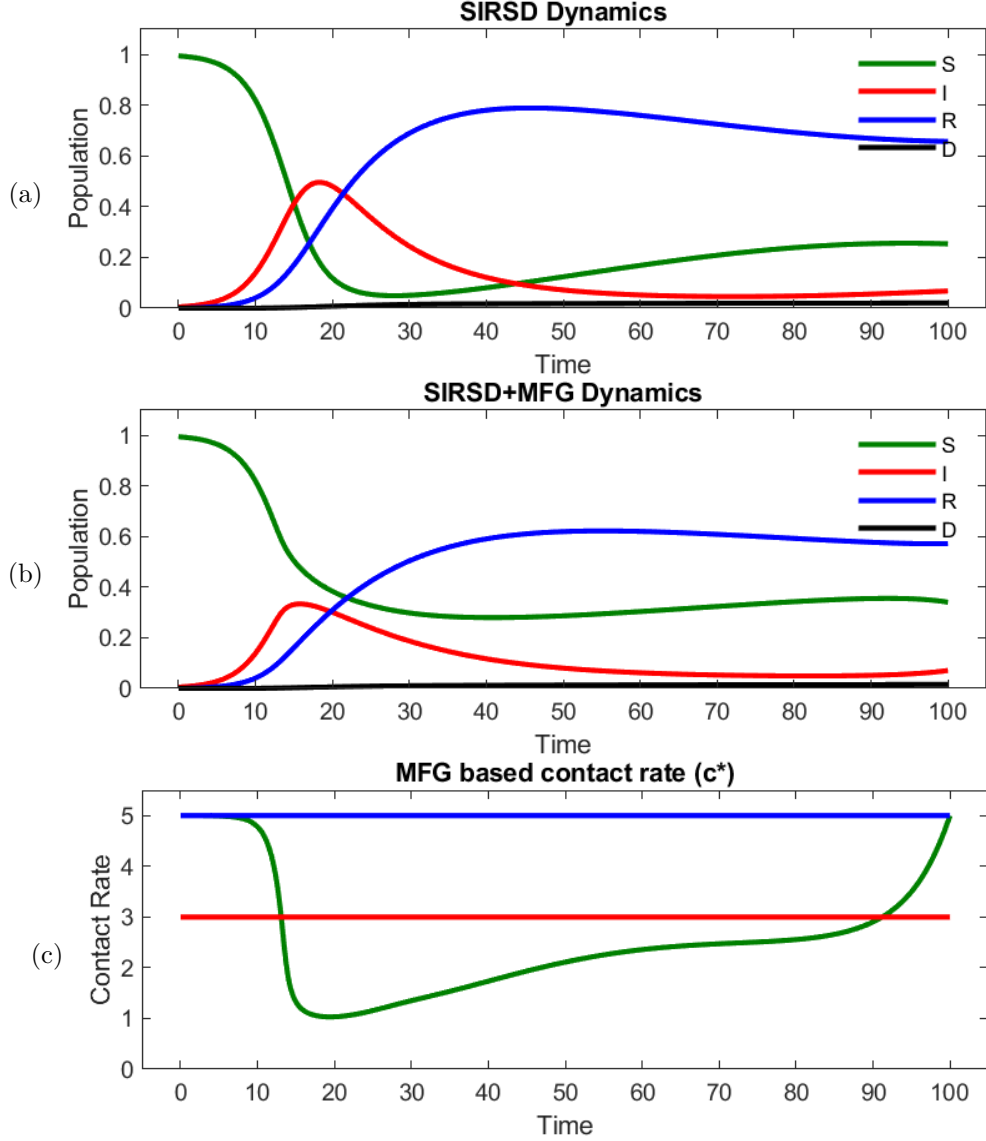


**Figure 3:** Basic SIRSD epidemic dynamics (top) and mean field game epidemic dynamics (middle) for an initial infected population of  $I_0 = 0.005$  or  $0.5\%$ . The optimal contact rate for the optimizing populations in the MFG + SIRSD model is displayed in the bottom row. Computed for the time horizon  $T = 100$ .

are generally lower and happen earlier in the case of Optimizers, since their strategic/selfish behavior decreases the effective reproductive number. Interestingly, for relatively low  $I_0$ , the Susceptible Optimizers' contact rate remains high at first (to avoid impacting their lifestyle satisfaction/instantaneous utility while the probability of catching the infection is still fairly low) and decreases rapidly once the proportion of Infected reaches some threshold.

Turning to dependence on the recovery rate  $\mu$  (Figure 5), we now see a significant qualitative difference

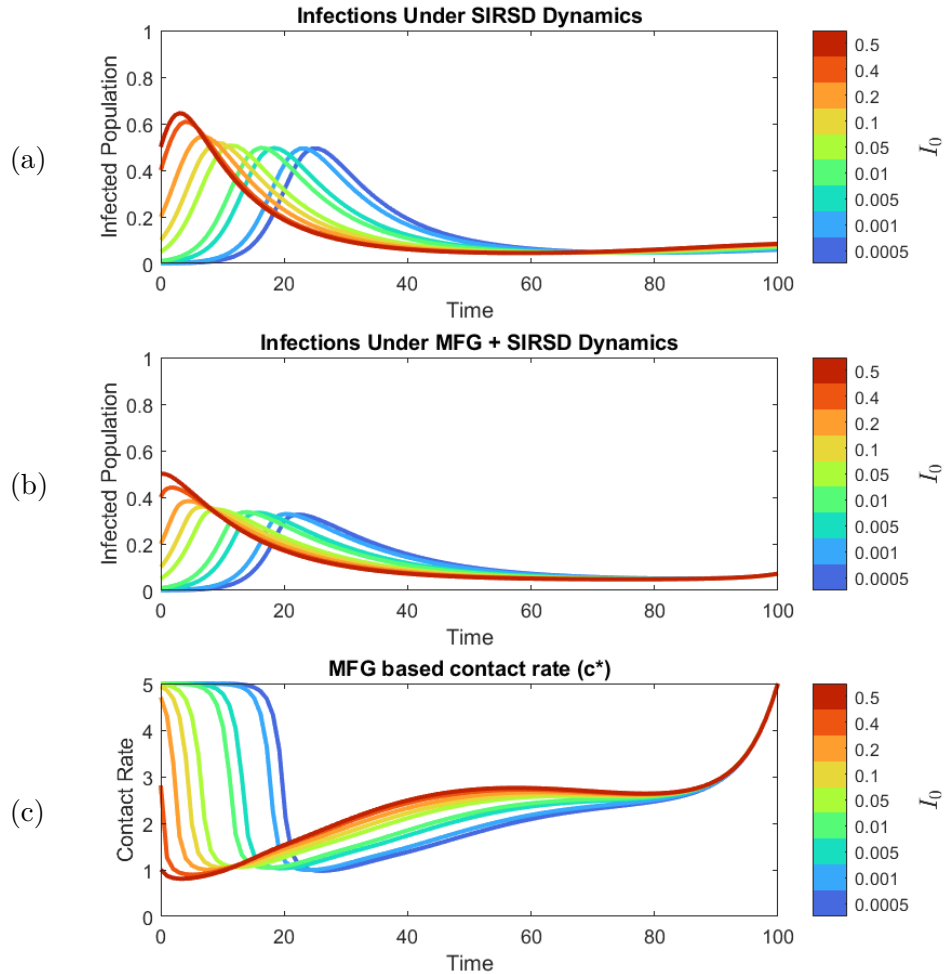


**Figure 4:** Varying  $I_0$ , the initial proportion of infected in the population. Infected populations for SIRSD (top) and MFG+SIRSD (middle) and the optimal contact rates (bottom) for various  $I_0$ .

between the two scenarios. In the traditional SIRSD (or “Reckless only”) model, the peak of infection increases monotonically as  $\mu$  decreases, since Infected individuals now have a longer time to infect others. A more complicated and largely the opposite trend holds for the population of Optimizers. Ignoring the late increase just before the end (driven by our lack of terminal penalty for being ill), the peak of infection first increases as  $\mu$  varies from  $\frac{1}{2}$  to  $\frac{1}{10}$ , and the reasons for this are the same as in the above “traditional SIRSD” scenario. But from there on (as  $\mu$  decreases further and the expected time to recovery increases correspondingly), the peak of infection decreases significantly because Susceptible Optimizers respond to the risk of prolonged illness with increasingly drastic reductions in contact rates. This phenomenon is also consistent with prior observations reported in [10] for an MFG-based SIR model with a density-based force of infection, no immunity waning, and

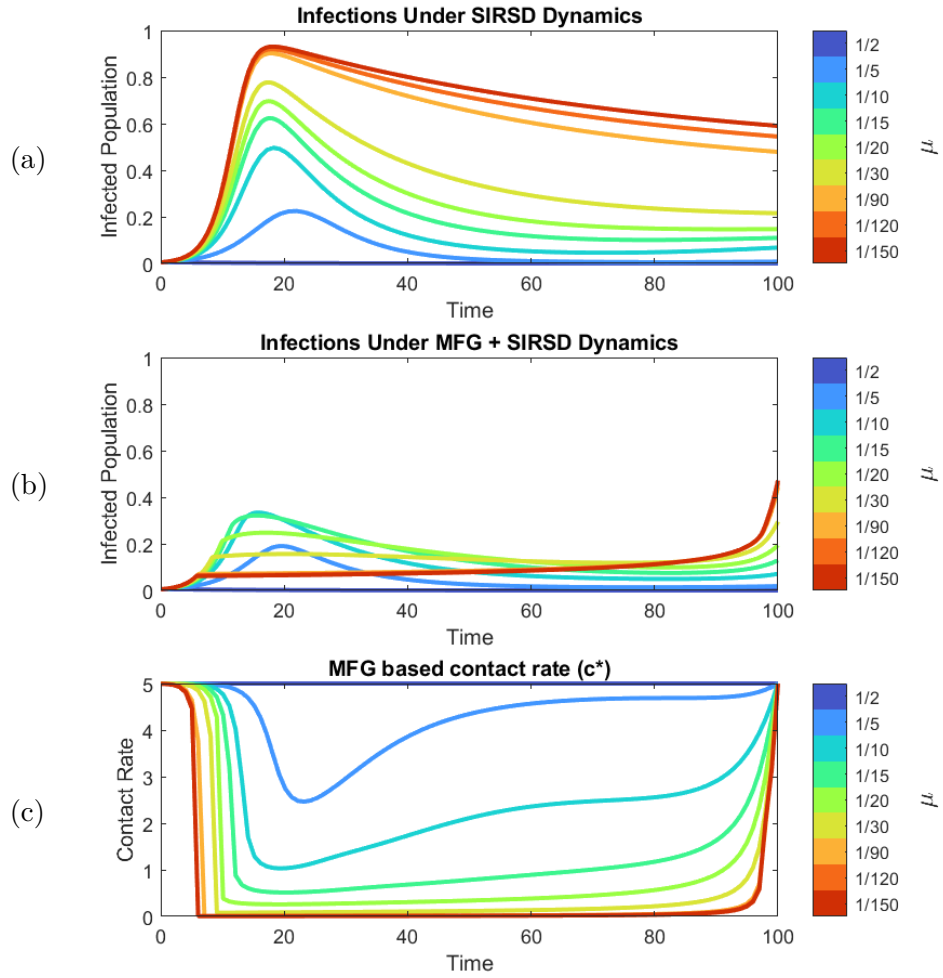


**Figure 5:** Varying the recovery rate  $\mu$ : a comparison of “Reckless only” and “Optimizers only” scenarios. Same format as in Fig. 4. The presented results correspond to the  $\gamma = 1/90$  vertical line in Figure 7.

no deaths.

A similar contrast is also clear when we vary the rate of immunity waning,  $\gamma$ ; see Figure 6. In traditional SIRSD models, shorter immunity (and larger  $\gamma$ ) leads to more infected individuals: a slightly higher peak and, much more noticeably, a higher  $I(t)$  long after that peak due to re-infections of many newly susceptibles. The latter is also true for the population of Optimizers, but the peak clearly decreases since it is driven by lower contact rates of Susceptible Optimizers, adopted in response to larger  $\gamma$ .

To provide a more intuitive summary of  $(\mu, \gamma)$ -dependence, we also include heatmaps in Figure 7, which show how varying these parameters affects the two main epidemics outcomes: the peak in-

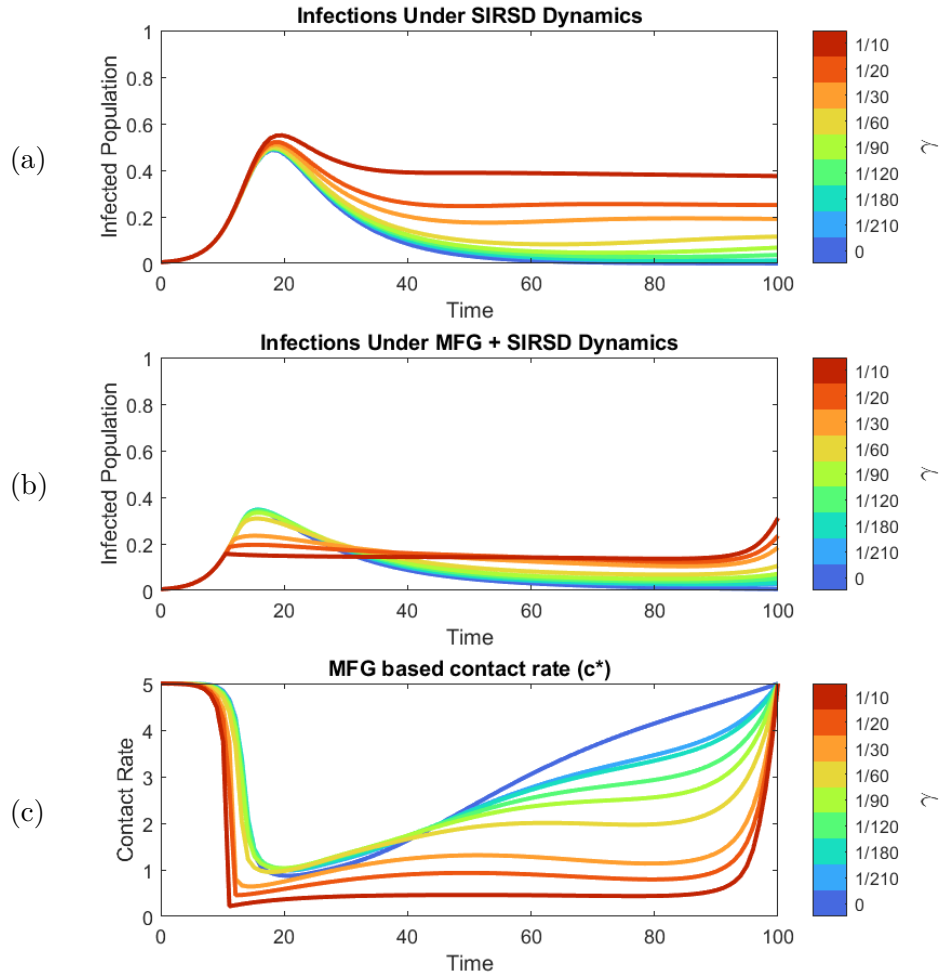


**Figure 6:** Varying the immunity waning rate  $\gamma$ : a comparison of “Reckless only” and “Optimizers only” scenarios. Same format as in Fig. 4. The presented results correspond to the  $\mu = 1/10$  horizontal line in Figure 7.

fection fraction<sup>3</sup> and the total number of dead. Overall, the heatmaps show predictably monotone dependence of outcomes on these parameters for the classical SIRSD model and much better outcomes (but with a clear non-monotonicity) in the MFG model due to Optimizers’ strategic behavior.

We end this two-scenario comparison by varying the “high mortality rate”  $\delta_2$ , which is in effect when the number of Infected individuals exceeds a threshold ( $I(t) \geq d_2 = 0.25$ ). The results of these experiments are shown in Figure 8. The color of curves in subfigures (a)-(d) indicated the value of  $\delta_2$ , with the darkest blue showing the case with a constant/low mortality rate ( $\delta(I) = \delta_2 = \delta_1 = 0.001$ )

<sup>3</sup> As Figures 5 and 6 show, for extremely low values of  $\mu$  and extremely high values of  $\gamma$ , our lack of terminal penalty for being ill at the time  $T$  can lead to late infection outbreaks under MFG dynamics. To prevent this issue from obscuring the comparison, in Figure 7 the “peak infection fraction” is defined as  $\max_{t \in [0, T/2]} I(t)$ .

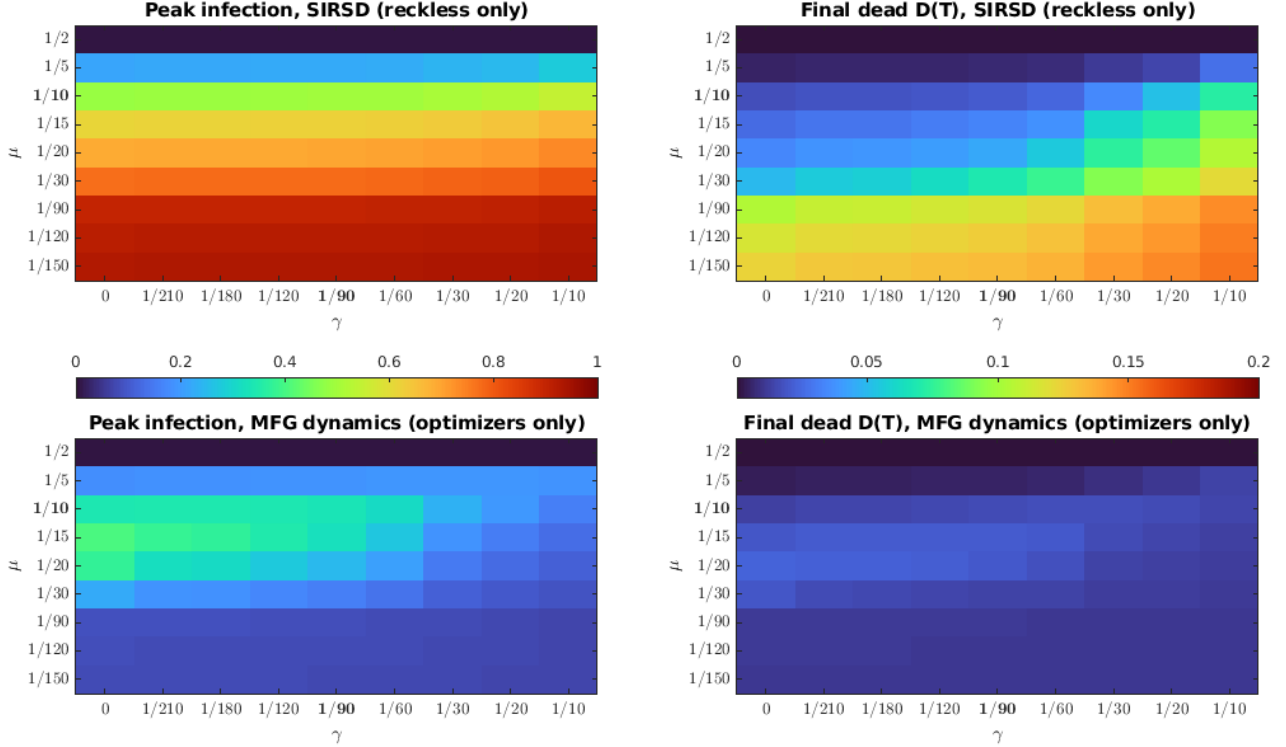


**Figure 7:** Epidemics outcomes varying in response to changes in parameters  $\gamma$  (the immunity waning rate) and  $\mu$  (the recovery rate). The peak of infection (defined as  $\max_{t \in [0, T/2]} I(t)$ ) is shown on the left while the total number of dead  $D(T)$  is shown on the right. The top row corresponds to the “classical SIRSD” dynamics, which is equivalent to the “everyone is Reckless” scenario in our model. The bottom row corresponds to the “pure MFG-SIRSD” dynamics, which is equivalent to the “everyone is an Optimizer” scenario in our model. The axis are not uniformly scaled, with the sampled parameter values corresponding to epidemics trajectories shown in subsequent figures. In particular, the row  $\mu = 1/10$  corresponds to Fig. 5 while the column  $\gamma = 1/90$  corresponds to Fig. 6.

and the next (light blue) curve corresponding to our default parameter value  $\delta_2 = 0.002$ .

As  $\delta_2$  grows, a traditional SIRSD model yields a much lower number of currently Infected individuals throughout the course of epidemic (subfigure (a)) since so many of them die (subfigure (e)) when  $I(t)$  is sufficiently high. (We recall that, based on (2), the mortality rate starts to increase significantly from  $\delta_1 = 0.001$  towards  $\delta_2$  once  $I(t)$  exceeds a lower threshold  $d_1 = 0.15$ .) The peak of infection also decreases (as  $\delta_2$  grows) in the Optimizers-only scenario (subfigure (b)). But this is primarily driven by their sharp decrease in contact rates when  $I(t)$  is high (subfigure (c)), leading to a decrease in the mortality rate to  $\delta_1$  by the time  $t = 40$  even for the highest explored  $\delta_2$  values (subfigure (d)). As a result, the overall number of dead in this Optimizers-only scenario grows very slowly with  $\delta_2$ ; see Fig. 8(e).

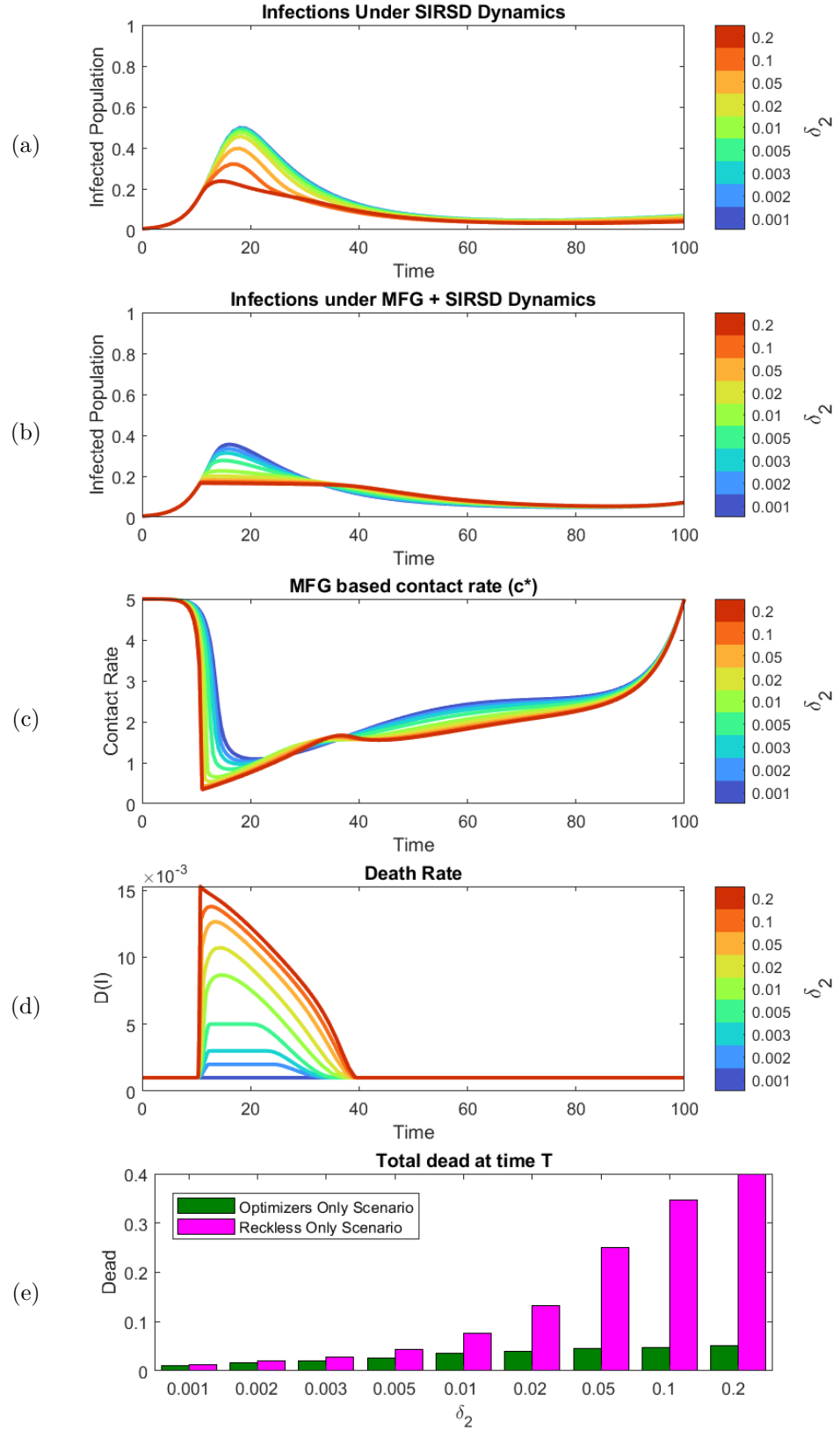


**Figure 8:** Varying the high-mortality rate  $\delta_2$ , which is only in effect when the infections are high ( $I > d_2$ ). (a) Infected as a function of time for the Reckless-only scenario. The next three subfigures correspond to the Optimizers-only scenario showing the time-dependent number of Infected in (b), contact rate of Susceptible Optimizers in (c), and the death rate  $\delta(I(t))$  in (d). The overall numbers of dead under both scenarios are compared in (e).

### 3.2 Different behavioral patterns

In this subsection we explore the impact of different behavioral patterns (subpopulations of Reckless, Followers, and Optimizers) and behavioral switches on the course of epidemics. Focusing first on the simplified scenario of no switches ( $\lambda_{j,k} = 0$  for all  $j, k \in \{r, f, o\}$ ), we consider the basic interactions between the two subpopulations considered before: the Reckless and Optimizers (for now, assuming that  $S_f(0) = I_f(0) = R_f(0) = 0$ ). The key parameter here will be  $\rho_r \in [0, 1]$ , the initial fraction<sup>4</sup> of Reckless in the population. Since the Followers are absent and we assume proportional representation among those initially infected, this means that  $I_r(0) = \rho_r I(0)$ ,  $I_o(0) = (1 - \rho_r)I(0)$ ,  $S_r(0) = \rho_r S(0)$ ,  $S_o(0) = (1 - \rho_r)S(0)$  with  $R(0) = 0$  and  $S(0) = 1 - I(0)$ . As we show in Figure 9, when the higher proportion of the population is Reckless,

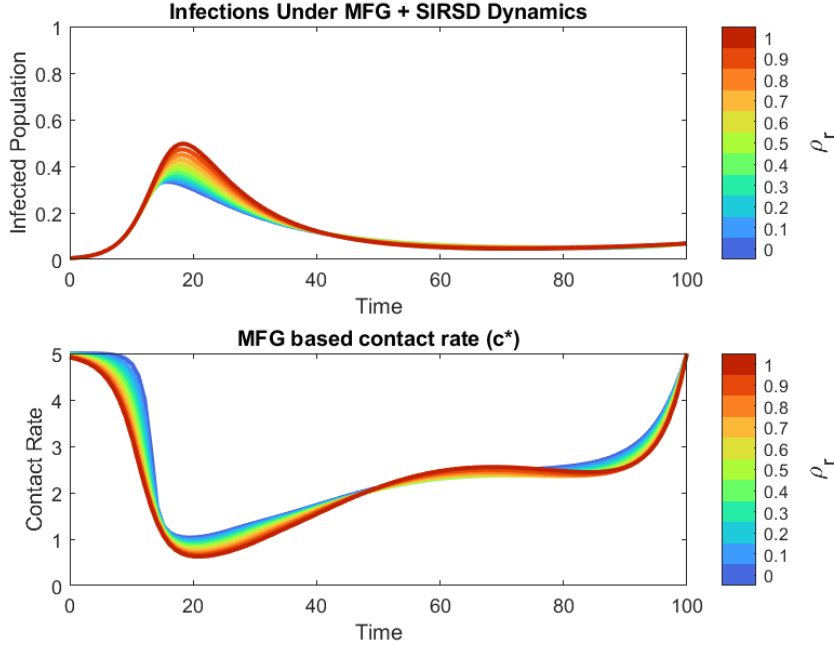


**Figure 9:** Varying the initial share of Reckless individuals ( $\rho_r \in [0, 1]$ ) in a “Reckless and Optimizers” scenario without behavioral switches. (a) Total infected population  $I(t)$ . (b) Contact rate of Susceptible Optimizers,  $c^*(t)$ . The colors of curves indicate the  $\rho_r$  values. The dark blue curves correspond to a traditional MFG-SIRSD model – a homogeneous all-Optimizers population ( $\rho_r = 0$ ). The dark red  $I(t)$  curve corresponds to the traditional SIRSD model – a homogeneous all-Reckless population ( $\rho_r = 0$ ), while the dark red  $c^*(t)$  curve shows the contact rate that a single Susceptible Optimizer would use (if added to this scenario, with no hope of affecting the course of epidemic).

the total number of Infected individuals (and the peak of infection) become higher as well, despite

<sup>4</sup>In all experiments without behavioral switching, the fractions of subpopulations can only change over time due to mortality differences resulting from their different contact rates.

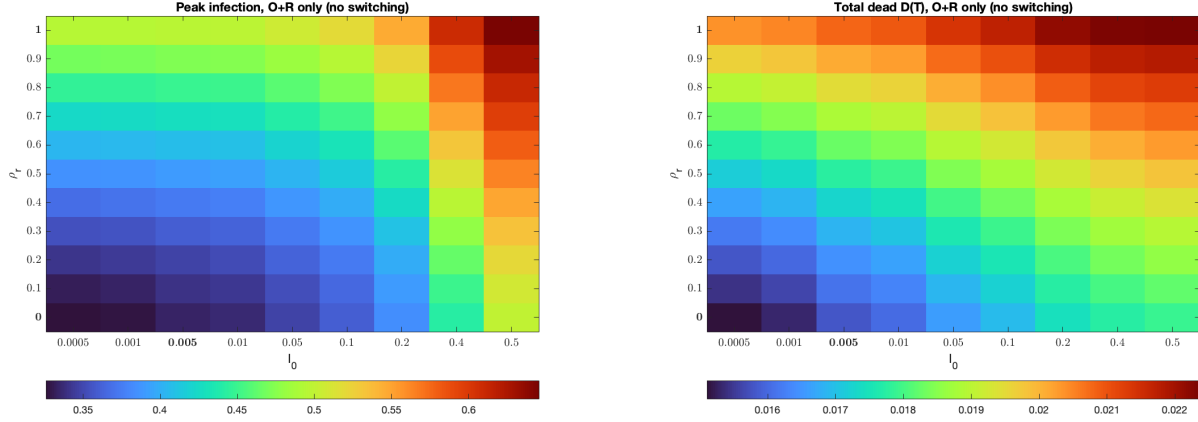


**Figure 10:** Epidemics outcomes varying in response to changes in parameters  $I_0$  (the initial fraction of Infected, spread proportionally between the two behavioral subpopulations: Reckless and Optimizers) and  $\rho_r$  (the initial fraction of Reckless). The peak of infection (defined as  $\max_{t \in [0, T/2]} I(t)$ ) is shown on the left while the total number of dead  $D(T)$  is shown on the right. The axis are not uniformly scaled, with the sampled parameter values corresponding to epidemics trajectories shown in prior figures. In particular, the horizontal lines  $\rho_r = 0$  and  $\rho_r = 1$  correspond to Fig. 4 while the vertical line  $I_0 = 0.005$  corresponds to Fig. 9. Both response variables exhibit monotone dependence on each of these two parameters.

the Susceptible Optimizers' efforts (they generally adopt lower contact rates in response to higher  $\rho_r$ ). The effect on the total number of dead is similar. These conclusions also hold true for other initial fractions of Infected; see Figure 10.

We next consider the situation where 50% of people are initially Reckless and compare the impact of Optimizers depending on their initial fraction: either the remaining 50% (as shown in Figure 11(a)) or an even 25% to 25% split between the Optimizers and Followers (as shown in Figure 11(b)). Not surprisingly, the latter scenario results in a higher peak of infection and more deaths even though the Susceptible Optimizers adopt somewhat lower contact rates when half of them are replaced by Followers. The Susceptible Followers' contact rates (shown in yellow) are qualitatively interesting. They start fairly close to the Susceptible Reckless' rate  $\bar{c}_s$  (shown in magenta), since they are initially in the majority. But most of those Reckless become Infected quickly, so after  $t \approx 18$  Susceptible Optimizers (whose contact rate is shown in green) are in the majority and Susceptible Followers mimic them much more closely. This changes again as more Reckless individuals recover and start losing immunity, with the number of Susceptible Reckless and optimizers fairly comparable after

$t \approx 60$  and Susceptible Followers equally influenced by them.

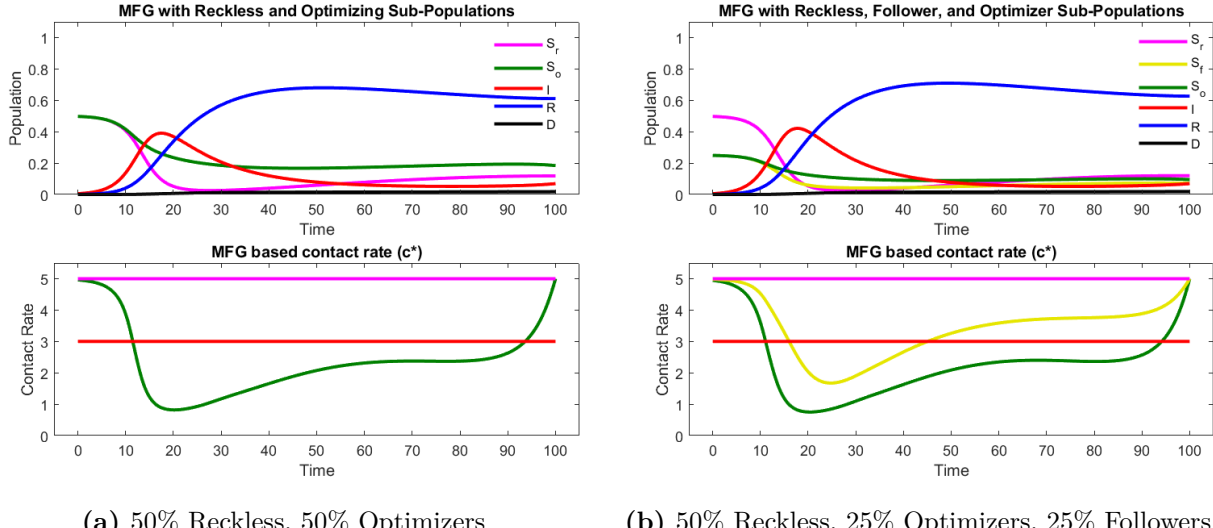
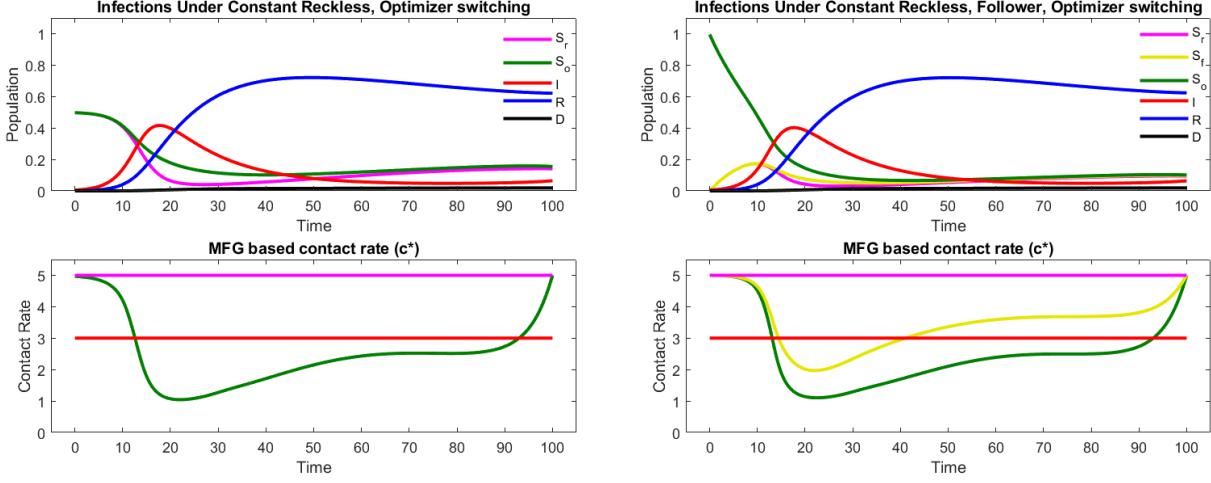


**Figure 11:** Two scenarios to highlight the importance of the initial fraction of Optimizers among the non-Reckless individuals (assuming no behavioral switches and that a half of population are initially Reckless). (a) All non-Reckless are Optimizers. (b) Non-Reckless are initially equally split between Optimizers and Followers. In the lower row, red indicates the contact rate of all Infected, while magenta, green, and yellow show the contact rates of Susceptible Reckless, Optimizers, and Followers respectively. The peak of infection is  $\approx 39\%$  in (a) and  $\approx 42.1\%$  in (b). The total number of dead is  $\approx 1.8\%$  in (a) and  $\approx 1.9\%$  in (b).

To illustrate the effect of behavioral switching, we first focus on constant switching rates and consider two different scenarios. In the first (shown in Figure 12(a)), the initial population consists of an equal number of Reckless and Optimizers, with an equal rate of switching between them ( $\lambda_{r,o} = \lambda_{o,r} = 1/30$ ) and no Followers ( $\lambda_{r,f} = \lambda_{o,f} = 0$ ). This is a switching-added modification of the example already presented in Figure 11(a). In the second scenario (illustrated in Figure 12(b)), the initial population consists of Optimizers only, while Reckless and Followers emerge later as a result of symmetric behavioral switching ( $\lambda_{j,k} = 1/30$  for all  $j \in \{r, f, o\}$ ,  $k \in \{r, f, o\} \setminus \{j\}$ ). This is a switching-added modification of our very first MFG example in Figure 3. Here, Subpopulations of Reckless and Followers grow quickly due to this behavioral switching. Followers start by imitating Optimizers (who comprise most of the population for small  $t$ ), but later use the contact rate much closer to  $(c_{s,o}^*(t) + \bar{c}_s)/2$ . In both scenarios, behavioral switches make it harder for the Optimizers to lower the peak of infection. Indeed, the maximum fraction of simultaneously Infected is  $\approx 41.6\%$  in Fig. 12(a) compared to  $\approx 39\%$  in Fig. 11(a); and also  $\approx 40.2\%$  in Fig. 12(b) compared to  $\approx 33.4\%$

in Fig. 3(b).



(a) 50% Reckless + 50% Optimizers to start,  $R \leftrightarrow O$  switching only, at rate 1/30

(b) 100% Optimizers to start, all switching rates = 1/30

**Figure 12:** Two scenarios with constant switching rates: (a) Reckless and Optimizers only, initially at 50% each, with an equal rate of switching between them ( $\lambda_{r,o} = \lambda_{o,r} = 1/30$ ) and no Followers; cf. Fig. 11(a). (b) Starting from Optimizers only, but with all six switching rates set to  $\lambda = 1/30$ ; cf. Fig. 3(bc).

For our final example presented in Figure 13, we return to the 2-sub-populations setting (Reckless and Optimizers only) and explore the effect of non-constant behavioral switching by Optimizers. In particular, we use

$$\lambda_{o,r} = \frac{1}{30} (1 - I(t)) \left( 1 + \alpha \left[ \bar{u}_s - u(c_{s,o}^*(t)) \right] \right), \quad (37)$$

where  $\alpha \geq 0$ . The factor  $(1 - I)$  models their lowered likelihood of switching to Reckless behavior when the proportion of infected people is high. The last factor models an increased likelihood of becoming Reckless due to fatigue/frustration (since the chosen Nash-optimal contact rate lowers one's instantaneous utility). To simplify the interpretation, we keep the rate of the reverse (" $R \rightarrow O$ ") switching constant with  $\lambda_{r,o} = \frac{1}{30}$ .

When  $\alpha = 0$ , the case shown by the lowest (dark blue) curves in Figure 13, the fatigue/frustration has no influence, and " $O \rightarrow R$ " switching is only decreased when the Infection is high. This decrease makes it slightly easier for the Optimizers to lower the peak of infection compared to Figure 12(a). But for  $\alpha > 0$ , the Susceptible Optimizers face an interesting dilemma: a lower contact rate decreases the probability of getting Infected in the near term, but increases the chances of switching to Reckless

behavior (and hence also the chances of getting Infected in the future). As shown in Fig. 13(b), higher  $\alpha$  values force them to adopt higher contact rates, which leads to a higher proportion of Infected for  $t \in [15, 35]$ ; see Fig. 13(a). Nevertheless, they still use a noticeably lower contact rate near the peak of Infection. For higher  $\alpha$  values, there is also a significant decrease of contact rates near the end of the planning interval. Even though this results in a spike in “ $O \rightarrow R$ ” switching shown in Fig. 13(c), our lack of terminal penalty for being sick at the time  $T$  makes this strategy advantageous – in those few remaining days, Optimizers would still prefer not to become Infected but are far less concerned with becoming Reckless.

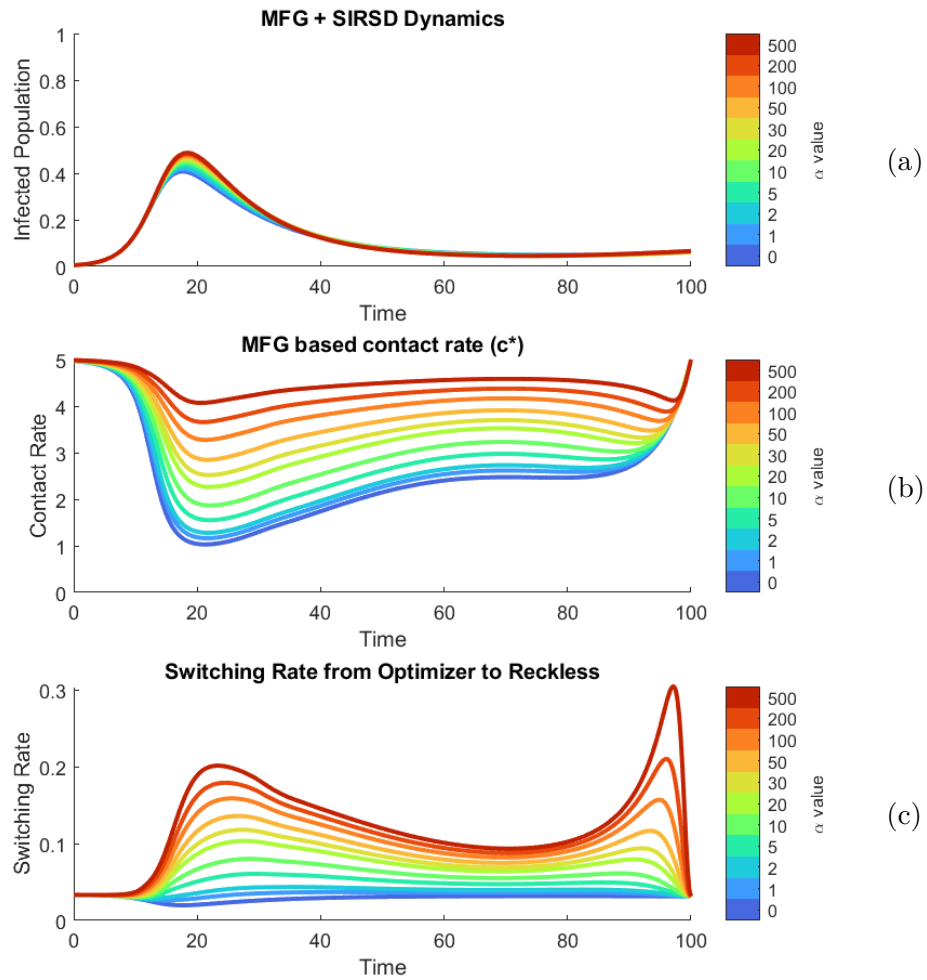


**Figure 13:** Varying the exponent  $\alpha$  in the “Optimizers to Reckless” switching rate function. (a) Infected population, (b) optimal contact rates, and (c)  $O \rightarrow R$  switching rates all shown as a function of time for various  $\alpha$  starting from an initial population that consists of 50% Reckless, 50% Optimizers individuals.

## 4 Discussion

We have presented a behavioral-epidemiological model, in which a part of the population (the Optimizers) are highly rational in choosing their contact rate while others either stick to their usual life pattern (the Reckless/stubborn) or highly influenced by others, preferring a Susceptible-population-averaged contact rate (the Followers/consensus-seekers). Importantly, each Optimizer makes their choice keeping in mind the behavior of other (non-rational) sub-populations, the game-theoretic aspects (i.e., all Optimizers are making that choice simultaneously and thus affecting each other), the human propensity to switch occasionally to different behavioral patterns, and the effects on the future epidemics trajectory of all of the above. Their optimal (Nash-equilibrium) choice is modeled in the framework that extends the more usual approach of multi-population MFGs. Since there are finitely many (health, behavioral) states, this model yields a two point boundary value problem for a system of ODEs, which is readily solvable by standard numerical methods.

Our results in § 3 confirm that selfish/independent decision makers can significantly reduce the peak infection count. This is consistent with prior findings in Optimizers-only MFG models [1, 2, 10]. This “flattening of the curve” also helps to reduce the number of disease-induced deaths, especially so if the mortality rate increases sharply when the number of Infected individuals exceeds some threshold. We also show that the presence of other (non-rational) sub-populations can significantly limit the ability of Optimizers to produce this positive effect, even when they stick to much lower contact rates. Qualitatively, this fact is not surprising (particularly when there are many Reckless individuals), but our model allows to quantify this difference. We also find that the impact of Followers depends on the relative abundance of Optimizers versus Reckless among those currently Susceptible. Near the peak of the epidemic, when the higher percentage of Reckless are Infected or recently Recovered, the Susceptible Followers tend to be heavily influenced by Optimizers and thus more careful. But this is partly due to our modeling assumption that their reference group are only those currently Susceptible.

There are several obvious extensions that would be relatively easy to implement, including other epidemiological compartment models, more sub-population types with different behavioral logic (e.g.,

semi-Reckless, who stick to a specific reduced contact rate level), effects of vaccinations, and different (e.g., health-state-dependent or peer-pressure-induced) behavioral switching rates. An extension to “graphon-structure” MFGs [1] would be also natural to model the effects of travel restrictions and the age/frailty spectrum in the population.

It will be harder but certainly useful to include a refined model of fatigue-induced behavioral switches. Our simplified version presented here (based on the instantaneous utility reduction) ignores the build up of fatigue over time. In that sense, we model more of a current-life-style-frustration than adherence fatigue here. It would be also very useful to consider the effects of uncertainty (e.g., on duration of immunity, vaccine efficacy, or emergence of new viral strains) and partial or delayed information (e.g., about the current number of Infecteds) on Optimizers’ contact-rate choices and epidemiological consequences. Mean field control [10] and Stackelberg game [2] versions will be also clearly of interest for such behaviorally-heterogeneous populations. Another important next step will be to verify that such behaviorally-enriched MFG models are better at matching the real data from past epidemics.

On the fundamental level, MFGs make an important contribution to epidemiological literature by bringing rational choice of individuals to bear on the epidemic trajectory. But prior MFG models take this to an extreme by assuming that *everyone* is fully informed, perfectly rational, capable of long-term foresight, and consistent in carrying out their plans. Here, we relaxed several of these limitations, but our assumptions about the cognitive abilities and self-awareness of Optimizers are still rather idealized. It would be useful to develop models of “time-limited” rationality or rationality based on limited/local information, perhaps in the spirit of what was already proposed in MFG-models of crowd dynamics in traffic engineering [8, 12].

To those used to rational decision theory, it might be tempting to seek a rational explanation for the behavior of each subpopulation; e.g., a question about different utility functions that could rationalize the behavior of Reckless or Follower individuals could be viewed as an inverse problem for multi-population MFGs [39]. But we believe that such rationalizations would have limited practical impact in epidemiological context, and that it is more useful to admit that some (and perhaps most) humans are not making decisions based on game-theoretic considerations. This is already well-recognized in epidemiological literature, particularly in papers on individual vaccination decisions. While the

classical game-theoretic models typically predict that herd immunity is unachievable without strong governmental policy [3, 18], there is also empirical evidence that vaccination decisions are often not “strategic” and that, at least with seasonal influenza vaccinations, individuals often disregard others’ decisions when making their own [38]. This is why more recent work also includes a number of models where choices are based on cognitive biases, various rules of thumb, and inertia [34, 37, 43]. Similarly, it is clear that non-rational decision making also plays a role in social distancing decisions and thus should be carefully considered in contact rate modeling.

Finally, we must acknowledge that the model presented here remains primarily qualitative in nature. To build accurate predictive models that would be suitable for evaluating policy proposals, descriptions of non-rational behavioral patterns and the switching rate functions should be developed in a close collaboration with domain experts: epidemiologists, social psychologists, and behavioral economists. More generally, we hope that incorporating behavioral patterns and collaborating with domain experts will also improve the predictive power of MFGs as generative models of human behavior in other critical scenarios with complex social interactions (e.g., evacuating a building in case of emergency, retail investors reacting to major market news, dynamics of labor markets in the face of disruptive technologies, etc).

## Acknowledgments

This research was partially funded by the National Science Foundation (award DMS-2111522) as well as the Air Force Office of Scientific Research (award FA9550-22-1-0528) and the second author’s Royal Society Wolfson Visiting Fellowship. A part of this work was done during the second author’s sabbatical year at Imperial College London (ICL), and he is thus grateful to ICL for its hospitality. The authors also thank A. Gumel for pointing out many relevant papers and S. Ellner for useful suggestions on improving this manuscript.

## Data and Code Availability

All data and code used to generate the figures in this manuscript will be available online at <https://github.com/eikonal-equation/Behavioral-MFGs-in-epidemiology>.

## References

- [1] Aurell, A., Carmona, R., Dayanikli, G. & Lauriere, M. (2022) Finite state graphon games with applications to epidemics. *Dynamic Games and Applications* **12**, 49–81.
- [2] Aurell, A., Carmona, R., Dayanikli, G. & Lauriere, M. (2022) Optimal incentives to mitigate epidemics: a Stackelberg mean field game approach. *SIAM J. Control Optim.* **60**, S294–S322.
- [3] Bauch, C.T. & Earn, D.J. (2004) Vaccination and the theory of games. *Proceedings of the National Academy of Sciences* **101**, 13391–13394.
- [4] Bensoussan, A., Huang, T. & Lauriere, M. (2018) Mean field control and mean field game models with several populations. *arXiv preprint arXiv:1810.00783* .
- [5] Brémaud, L. (2024) *Mean-Field Game description of virus propagation*. Ph.D. thesis, Université Paris-Saclay.
- [6] Bremaud, L., Giraud, O. & Ullmo, D. (2025) Mean-field game approach to epidemic propagation on networks. *arXiv preprint arXiv:2501.14601* .
- [7] Cardaliaguet, P. & Hadikhanloo, S. (2017) Learning in mean field games: the fictitious play. *ESAIM: Control, Optimisation and Calculus of Variations* **23**, 569–591.
- [8] Carrillo, J.A., Martin, S. & Wolfram, M.T. (2016) An improved version of the Hughes model for pedestrian flow. *Mathematical Models and Methods in Applied Sciences* **26**, 671–697.
- [9] Chen, J., Espinoza, B., Chou, J., Gumel, A.B., Levin, S.A. & Marathe, M. (2025) A simple model of coupled individual behavior and its impact on epidemic dynamics. *Mathematical Biosciences* **380**, 109345.
- [10] Cho, S. (2020) Mean-field game analysis of SIR model with social distancing. *arXiv preprint arXiv:2005.06758* .
- [11] Cirant, M. (2015) Multi-population mean field games systems with Neumann boundary conditions. *Journal de Mathématiques Pures et Appliquées* **103**, 1294–1315.

[12] Cristiani, E., Priuli, F.S. & Tosin, A. (2015) Modeling rationality to control self-organization of crowds: an environmental approach. *SIAM Journal on Applied Mathematics* **75**, 605–629.

[13] Dayanikli, G. & Laurière, M. (2024) Multi-population mean field games with multiple major players: Application to carbon emission regulations. *2024 American Control Conference (ACC)*, pp. 5075–5081.

[14] Doncel, J., Gast, N. & Gaujal, B. (2022) A mean field game analysis of SIR dynamics with vaccination. *Probability in the Engineering and Informational Sciences* **36**, 482–499.

[15] Egeli, A., Adıgüzel, S., Kapıcı, Y., Güc, B., Yetkin Tekin, A. & Tekin, A. (2021) Risk-taking behavior in recovered COVID-19 patients. *Psychiatria Danubina* **33**, 107–113.

[16] Espinoza, B., Chen, J., Orr, M., Saad-Roy, C.M., Levin, S.A. & Marathe, M. (2025) The impact of risk compensation adaptive behavior on the final epidemic size. *Mathematical Biosciences* **380**, 109370.

[17] Ferrari, M.J., Perkins, S.E., Pomeroy, L.W. & Bjørnstad, O.N. (2011) Pathogens, social networks, and the paradox of transmission scaling. *Interdisciplinary perspectives on infectious diseases* **2011**, 267049.

[18] Geoffard, P.Y. & Philipson, T. (1997) Disease eradication: private versus public vaccination. *The American Economic Review* **87**, 222–230.

[19] Gomes, D.A., Mohr, J. & Souza, R.R. (2013) Continuous time finite state mean field games. *Applied Mathematics & Optimization* **68**, 99–143.

[20] Hethcote, H.W. & Van Ark, J.W. (1987) Epidemiological models for heterogeneous populations: proportionate mixing, parameter estimation, and immunization programs. *Mathematical Biosciences* **84**, 85–118.

[21] Hethcote, H.W. & Yorke, J.A. (2014) *Gonorrhea transmission dynamics and control*, vol. 56. Springer.

[22] Huang, M., Malhamé, R.P. & Caines, P.E. (2006) Large population stochastic dynamic games:

closed-loop McKean-Vlasov systems and the Nash certainty equivalence principle. *Commun. Inf. Syst.* **6**, 221–252.

- [23] Huang, Y., Zhang, L., Fu, J., Wu, Y., Wang, H., Xiao, W., Xin, Y., Dai, Z., Si, M., Chen, X. *et al.* (2023) COVID-19 vaccine hesitancy among patients recovered from COVID-19 infection in Wuhan, China: cross-sectional questionnaire study. *JMIR public health and surveillance* **9**, e42958.
- [24] Kaim, A. & Saban, M. (2022) Are we suffering from the Peltzman effect? Risk perception among recovered and vaccinated people during the COVID-19 pandemic in Israel. *Public Health* **209**, 19–22.
- [25] Kierzenka, J. & Shampine, L.F. (2008) A BVP solver that controls residual and error. *Journal of Numerical Analysis, Industrial and Applied Mathematics* **3**, 27–41.
- [26] Lasry, J.M. & Lions, P.L. (2006) Jeux à champ moyen. i–le cas stationnaire. *Comptes Rendus Mathématique* **343**, 619–625.
- [27] Lasry, J.M. & Lions, P.L. (2006) Jeux à champ moyen. ii–horizon fini et contrôle optimal. *Comptes Rendus. Mathématique* **343**, 679–684.
- [28] Lauriere, M. (2021) Numerical methods for mean field games and mean field type control. *arXiv preprint arXiv:2106.06231* .
- [29] LeJeune, L., Ghaffarzadegan, N., Childs, L.M. & Saucedo, O. (2024) Mathematical analysis of simple behavioral epidemic models. *Mathematical Biosciences* **375**, 109250.
- [30] LeJeune, L., Ghaffarzadegan, N., Childs, L.M. & Saucedo, O. (2025) Formulating human risk response in epidemic models: Exogenous vs endogenous approaches. *European Journal of Operational Research* **324**, 246–258.
- [31] Martcheva, M., Tuncer, N. & Ngonghala, C.N. (2021) Effects of social-distancing on infectious disease dynamics: an evolutionary game theory and economic perspective. *Journal of Biological Dynamics* **15**, 342–366.
- [32] Nguyen, M.M., Freedman, A.S., Cheung, M.A., Saad-Roy, C.M., Espinoza, B., Grenfell, B.T.

& Levin, S.A. (2025) The complex interplay between risk tolerance and the spread of infectious diseases. *Journal of the Royal Society Interface* **22**, 20240486.

[33] Nold, A. (1980) Heterogeneity in disease-transmission modeling. *Math. Biosci.* **52**, 227–240.

[34] Oraby, T. & Bauch, C.T. (2015) Bounded rationality alters the dynamics of paediatric immunization acceptance. *Scientific reports* **5**, 10724.

[35] Oveson, A., Girvan, M. & Gumel, A.B. (2025) Modeling the impact of hospitalization-induced behavioral changes on the spread of COVID-19 in New York City. *Infectious Disease Modelling* **10**, 1055–1092.

[36] Pant, B., Safdar, S., Santillana, M. & Gumel, A.B. (2024) Mathematical assessment of the role of human behavior changes on SARS-CoV-2 transmission dynamics in the United States. *Bulletin of mathematical biology* **86**, 92.

[37] Papst, I., O’Keeffe, K.P. & Strogatz, S.H. (2022) Modeling the interplay between seasonal flu outcomes and individual vaccination decisions. *Bulletin of mathematical biology* **84**, 36.

[38] Parker, A.M., Vardavas, R., Marcum, C.S. & Gidengil, C.A. (2013) Conscious consideration of herd immunity in influenza vaccination decisions. *American journal of preventive medicine* **45**, 118–121.

[39] Ren, K., Soedjak, N. & Wang, K. (2025) Unique determination of cost functions in a multipopulation mean field game model. *Journal of Differential Equations* **427**, 843–867.

[40] Roy, A., Singh, C. & Narahari, Y. (2023) Recent advances in modeling and control of epidemics using a mean field approach. *Sādhanā* **48**, 207.

[41] Smith, J.M. (1982) Evolution and the Theory of Games. *Did Darwin get it right? Essays on games, sex and evolution*, pp. 202–215, Springer.

[42] Tembine, H. (2020) COVID-19: data-driven mean-field-type game perspective. *Games* **11**, 51.

[43] Voinson, M., Billiard, S. & Alvergne, A. (2015) Beyond rational decision-making: modelling the influence of cognitive biases on the dynamics of vaccination coverage. *PLOS One* **10**, e0142990.